A Study on the Superposition Method to Estimate the Ultimate Strength of Steel Reinforced Concrete Column Subjected to Axial Thrust and Bending Moment Simultaneously

By Takeshi NAKAMURA and Minoru WAKABAYASHI

(Manuscript received October 3, 1976)

Abstract

In this paper, considered is the further applicability of the "Superposition Method" to estimate the load carrying capacity of steel reinforced concrete column subjected to axial thrust and bending moment. The accuracy of the superposition method is checked in the combination use of various grades of concrete and steel. It is confirmed that the unsafe-side error of superposition method is not large even though steel portion with shallow depth is put in a cross section of a column and/or an asymmetrical steel shape is used, provided that the yield strength of steel is not too high. The unsafeside error of the superposition method is reasonably compensated by the reduction of ultimate strength of concrete which was specified in the design standard of AIJ for SRC structures.

1. Introduction

Steel reinforced concrete structural system (concrete encased steel structural system) was imported from the West at the end of The Meiji Period. At present, it is one of the most frequently used structural systems for the design of building structures in Japan. Steel reinforced concrete structures (SRC-structures) have the engineering properties of two elemental structural systems; ordinary reinforced concrete structural system and steel structural system. In this system, these two elemental structural systems compensate each other. The property of brittle failure caused by the material property of concrete is offset by the ductile property of steel. On the other hand, the weakness of steel against fire and high temperature is reinforced by an outer concrete encasement.

In Japan, strong earthquakes frequently occur. Under such severe natural circumstances, a steel reinforced concrete structural system has been developed as the most effective earthquake-resistant-structural system. Until quite lately, SRC system has been applied to design most high-rise building structures with more than six stories. Although a number of pure steel structures has been recently increasing since lightweight fire-proof material was developed and accepted by laws, the SRC system is still the most frequently used system for building structures about 45 m high and for the lower or underground portions of steel high-rise buildings.

The design formulas for beams and columns of SRC structures has been based on the so-called "Superposition Method" since the first design specification for steel reinforced concrete structures was completed by the Architectural Institute of Japan (AIJ) in 1958. The "Superposition Method" is based on the consideration that the

ultimate load carrying capacity of SRC structural elements is given by the sum total of the ultimate load carrying capacity of the individual elements which compose the SRC section, i.e., ordinary reinforced concrete and steel portion. It has been verified under the plasticity theory that the load carrying capacity of a composite structure composed of two or more components with different load carrying capacity is not smaller than the sum total of the load carrying capacity of the individual components[3),4)]. However, this verification is valid only for the component materials which behave in perfectly plastic manner. It has been confirmed in experiments that the value of the ultimate strain of concrete for crushing in compression is about 0.3～0.35%. It has been also understood that the "Superposition Method" to the load carrying capacity of the components composed of such materials does not give always the safeside estimation of load carrying capacity of a composite structure. When the depth of steel portion put in an SRC cross section is not very small in comparison with the depth of a resultant concrete section and ordinary low carbon steel with not very high yield strength ($_s\sigma_y$=2.4～3.3 t/cm^2) is put in the concrete with ordinary ultimate strength ($_c\sigma_0$=150～200 kg/cm^2), the unsafeside error of the "Superposition Method" is not so large that the application of that method becomes impossible. In such cases, the partial unsafeside error of the "Superpositions Method" is reasonably compensated by the use of the reduced ultimate strength of concrete. This reduction of concrete strength was taken into the specification to compensate for the imperfect casting of concrete due to the existence of steel portion and reinforcing bars which are complicatedly put in the SRC section and errors involved when the gross area of concrete cross section is used in the analysis.

Recently, high strength concrete and high strength steel have been developed to be used in the design of buildings. When high strength steel is used in the design of SRC structures, it is easily understood that the supperposition method does not give the safe-side value of the ultimate load capacity under pure compression if the yield limit strain of steel is larger than the crushing strain of concrete. In the combination use of concrete and high strength steel, a larger unsafe-side error of the superposition method would be anticipated. Further, the order and amount of the error of the superposition method has not been checked sufficiently for the case that the steel section with considerably smaller depth in comparison with the depth of concrete section is used. In this paper, the applicability of the superposition method for using high strength steel and the steel portion with the small depth in the SRC cross section are considered mainly.

2. General Description of the Superposition Method for the Ultimate Load Capacity of the SRC Column Section Subjected to Axial Thrust and Bending Moment

As previously mentioned, the principle of the superposition method is based on the consideration that the ultimate load carrying capacity of SRC structural elements is given by summing the load carrying capacity of the individual components, i.e.

reinforced concrete and steel. In order to help to understand, the fundamental superposition method is graphically shown in Fig. 1. The ordinate is axial thrust and the abscissa is bending moment. In the figure, the ultimate strength curves of plain concrete with rectangular cross section and pure steel portion with ideal I-section subjected to axial thrust and bending moment simultaneously are shown by chained line and dashed line, respectively. They are referred to as *M-N* interaction curves of concrete and steel portions, respectively. *M-N* interaction curve of SRC cross section by the superposition method is given by the envelope curve (dotted curve) of a group of curves which are obtained from making the origin of the *M-N* interaction curve of steel move on the *M-N* interaction curve of concrete. The equations to calculate the load capacity due to the superposition method is shown in section 4.

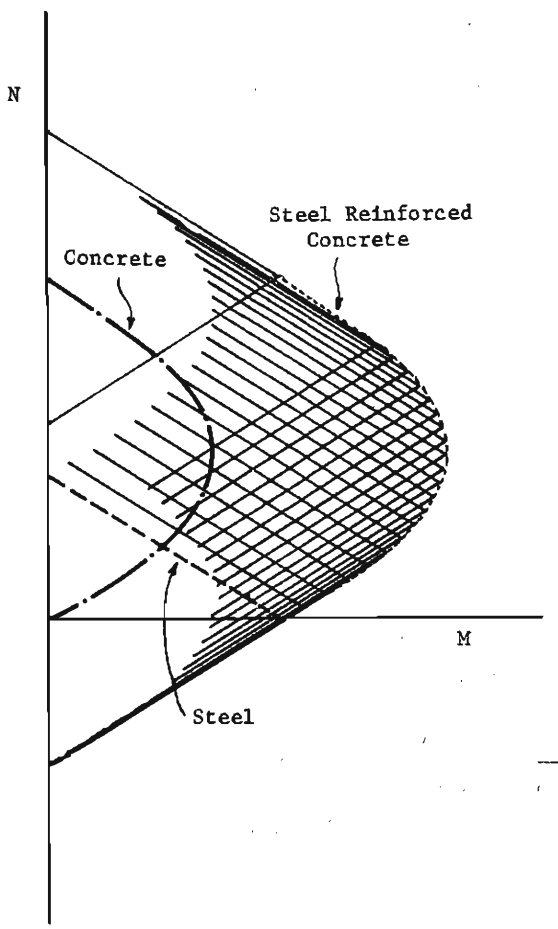

Fig. 1. Graphical Method of Superposition of Individual Component.

3. Calculation Method of the Ultimate Load Carrying Capacity of SRC Section Subjected to Axial Thrust and Bending Moment Simultaneously

The "Ultimate Strength Method" is well known as the most accurate method of calculation to obtain the ultimate load carrying capacity of SRC column section under axial thrust and flexure. The complete description of the "Ultimate Strength Method" is given in Refs. 1) and 2). Only the stress-strain relationship of concrete is different from that in Refs. 1) and 2). In this paper, the stress-strain relationship of concrete is assumed as shown in Fig. 2. Before the attainment of the maximum stress ${}_c\sigma_0$, the stress-strain relationship is parabolic. After the attainment of the maximum stress ${}_c\sigma_0$, the maximum value of stress ${}_c\sigma_0$ is maintained until the strain (${}_c\varepsilon_B$) reaches the value of $(1+\kappa)\cdot{}_c\varepsilon_0$, i.e. the crushing strain of concrete. In the strain range larger than $(1+\kappa)\cdot{}_c\varepsilon_0$, concrete can not sustain any load in compression. In tension range, concrete can not sustain any load. The stress-strain relationship of steel is assumed to be elastic-perfectly plastic in both tension and compression. The other main assumptions taken in this method of calculation are as follows. ① A plane of transverse section remains plane after deformation. ② The ultimate load carrying capacity of SRC section is attained when the strain in the extreme fiber of concrete in compression reaches the crushing value $(1+\kappa)\cdot{}_c\varepsilon_0$. It was confirmed by a number of experimental investigations in the past that the ultimate strength based on the assumption ② gives a good approximation to the real ultimate strength of a column section. Under the assumptions ① and ②, the strain distribution in a cross section at the ultimate state is easily obtained by giving the location of the neutral axis in flexure. Corresponding to the ultimate state of strain, the ultimate state of stress is calculated using the stress-strain relationships of the element materials. The ultimate load carrying capacity is obtained as the generalized stress resultants being in equilibrium with the ultimate state of stress. The results of the ultimate strength method are used to check the accuracy of the superposition method in this paper. The equations in the ultimate strength method are developed in the next section.

4. Method of Calculation

4.1 Assumed Stress-Strain Relationships

(1) Concrete (see Fig. 2(a))

In compression,

$$\left.\begin{aligned} \sigma &= {}_c\sigma_0\frac{\varepsilon}{{}_c\varepsilon_0}\left(2-\frac{\varepsilon}{{}_c\varepsilon_0}\right) && \text{for} \quad 0\leq\varepsilon\leq{}_c\varepsilon_0 \\ \sigma &= {}_c\sigma_0 && \text{for} \quad {}_c\varepsilon_0<\varepsilon\leq(1+\kappa)\,{}_c\varepsilon_0 \\ \sigma &= 0 && \text{for} \quad \varepsilon>(1+\kappa)\,{}_c\varepsilon_0 \end{aligned}\right\} \qquad \cdots\cdots(1)$$

In tension,

$$\sigma = 0 \qquad \cdots\cdots(2)$$

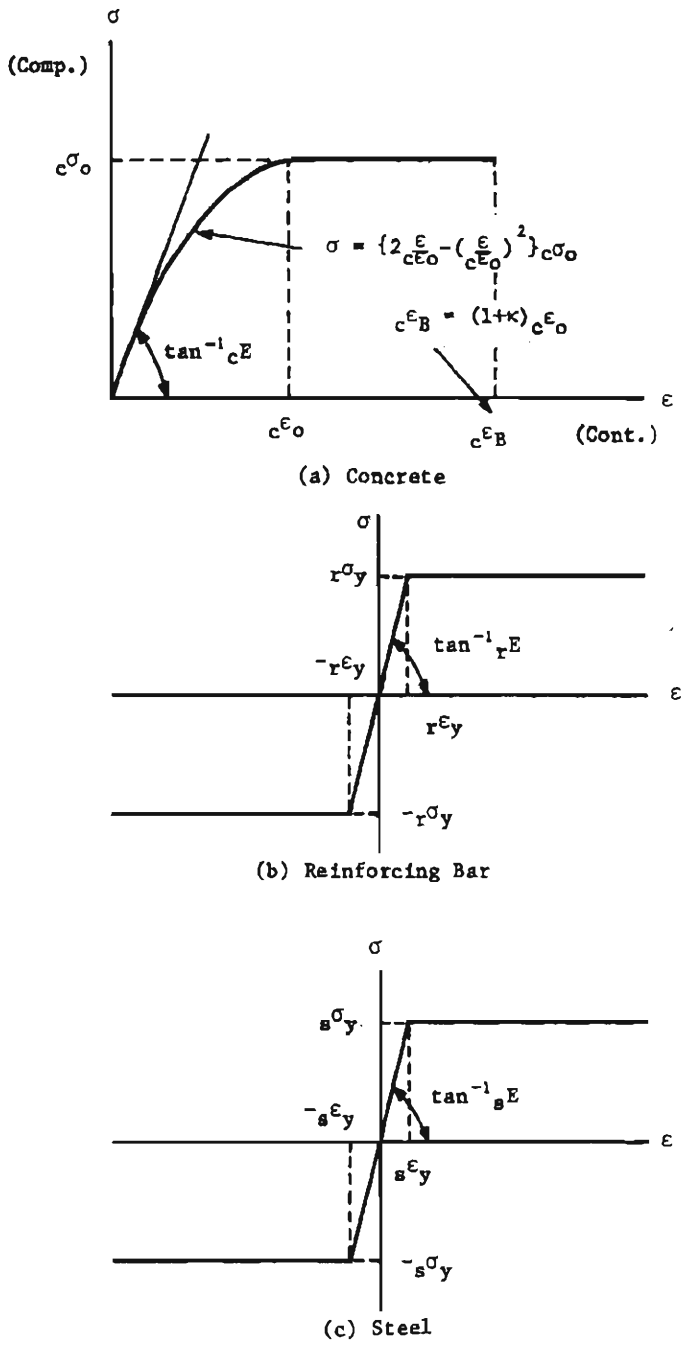

Fig. 2. Stress-Strain Relationships.

(2) Steel (see Figs. 2(b) and (c))

In both tension and compression

$$\left.\begin{aligned} \sigma &= {}_iE\varepsilon \qquad \text{for} \quad |\varepsilon| \leq {}_{ij}\varepsilon_y \\ \sigma &= {}_{ij}\sigma_y \qquad \text{for} \quad |\varepsilon| > {}_{ij}\varepsilon_y \end{aligned}\right\} \qquad \cdots\cdots(3)$$

where, $i=r, s, w$ and $j=1, 2, 3, \cdots$

4.2 Strain Distribution in a Cross Section at the Ultimate State

At the ultimate state, the strain in the extreme fiber of concrete in compression is assumed to be ${}_c\varepsilon_B=(1+\kappa)\,{}_c\varepsilon_0$, as shown in Fig. 3. Under the assumption ①, the strain in an arbitrary longitudinal fiber in a section is expressed in the next equation.

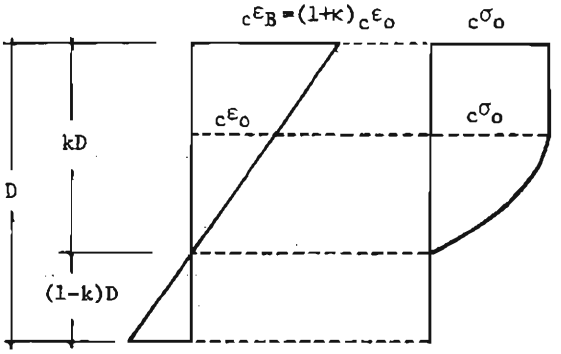

Fig. 3. Strain Distribution and Stress in Concrete at Ultimate State.

$$\left.\begin{aligned} {}_{ij}\varepsilon_c &= {}_c\varepsilon_B \frac{k-{}_{ij}d_c}{k} \\ {}_{ij}\varepsilon_t &= {}_c\varepsilon_B \frac{1-k-{}_{ij}d_t}{k} \end{aligned}\right\} \qquad \cdots\cdots(4)$$

where k is the location of the neutral axis in dimensionless form.

and $${}_{ij}d_c = \frac{{}_{ij}D_c}{D}$$

$${}_{ij}d_t = \frac{{}_{ij}D_t}{D}$$

$$i = r, s, w$$

$$j = 1, 2, 3, \cdots$$

r, s and w denote reinforcing bars, flange of the steel portion and the web of the steel portion, respectively. 1, 2, 3,$\cdots$ are the number of layers of steel and reinforcements. Corresponding to the strain distribution, the state of stress in a cross section is determined according to the stress-strain relationships. The definition of a sign of strain

and stress is that compressive strain and stress are positive in the fiber in the compression side of a section, and tensile strain and stress are positive in the fiber in the tension side.

4.3 *M-N* Interaction of Concrete Portion

M-N interaction curve of concrete portion at the ultimate state can be directly calculated under the assumptions ① and ②. The state of stress and the stress resultants at the ultimate state are shown in Fig. 4, with main geometrical values in a cross section. The resultant axial force N_c and bending moment M_c at the ultimate state are expressed as Eq. 5 expressed in a dimension of stress.

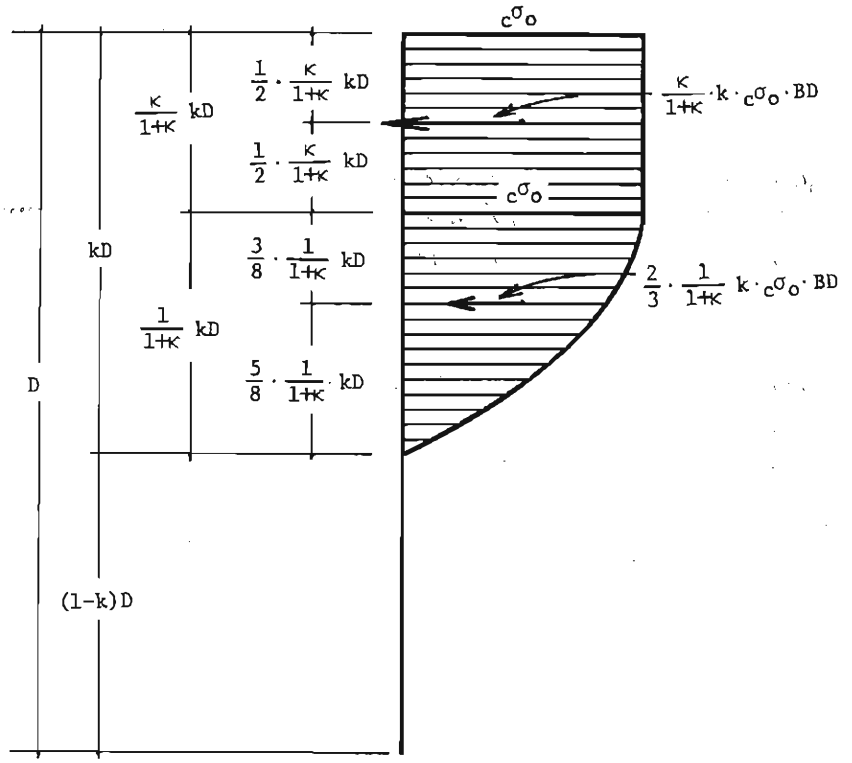

Fig. 4. Stress in Concrete at Ultimate State.

$$\left.\begin{aligned}\frac{N_c}{BD} &= \left(\frac{2}{3}\frac{1}{1+\kappa}+\frac{\kappa}{1+\kappa}\right)k_c\sigma_0 = \frac{2+5\kappa}{3(1+\kappa)}k_c\sigma_0 \\ \frac{M_c}{BD^2} &= \left\{\frac{2}{3}\frac{1}{1+\kappa}\left(\frac{1}{2}-k+\frac{5}{8}\frac{1}{1+\kappa}k\right)+\frac{\kappa}{2(1+\kappa)}\left(1-\frac{\kappa}{1+\kappa}k\right)\right\}k_c\sigma_0\end{aligned}\right\} \quad \cdots\cdots(5)$$

Equation 5 can be applied to the both cases of the superposition method and the ultimate strength method.

4.4 N and M of Reinforcing Bar and Steel Flange at the Ultimate State

Stress in a reinforcing bar or steel flange is exppressed as follows, corresponding to a strain shown in Fig. 5.

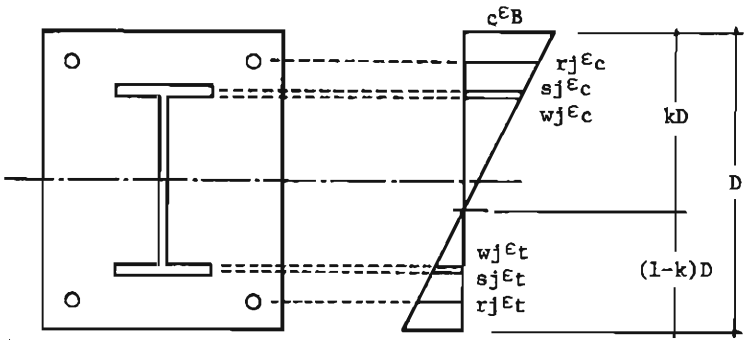

Fig. 5. Strain Distribution.

$$\left.\begin{aligned} {}_{ij}\sigma_c &= {}_{ij}E_{ij}\varepsilon_c && \text{for} && -{}_{ij}\varepsilon_y \leq {}_{ij}\varepsilon_c \leq {}_{ij}\varepsilon_y \\ {}_{ij}\sigma_c &= {}_{ij}\sigma_y && \text{for} && {}_{ij}\varepsilon_c > {}_{ij}\varepsilon_y \\ {}_{ij}\sigma_c &= -{}_{ij}\sigma_y && \text{for} && {}_{ij}\varepsilon_c < -{}_{ij}\varepsilon_y \end{aligned}\right\} \quad \cdots\cdots(6)$$

in compression side.

$$\left.\begin{aligned} {}_{ij}\sigma_t &= {}_{ij}E_{ij}\varepsilon_t && \text{for} && -{}_{ij}\varepsilon_y \leq {}_{ij}\varepsilon_t \leq {}_{ij}\varepsilon_y \\ {}_{ij}\sigma_t &= {}_{ij}\sigma_y && \text{for} && {}_{ij}\varepsilon_t > {}_{ij}\varepsilon_y \\ {}_{ij}\sigma_t &= -{}_{ij}\sigma_y && \text{for} && {}_{ij}\varepsilon_t < -{}_{ij}\varepsilon_y \end{aligned}\right\} \quad \cdots\cdots(7)$$

in tension side.

The resultant thrust ${}_{ij}N({}_{ij}N/BD)$ and moment ${}_{ij}M({}_{ij}M/BD^2)$ are obtained from these stresses, as follows.

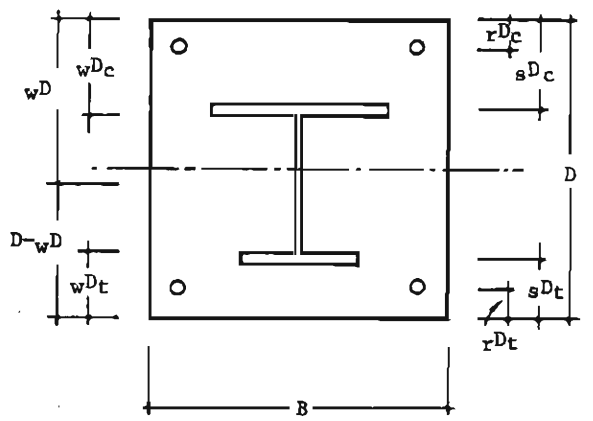

Fig. 6. Dimension of Cross Section.

$$\left.\begin{aligned}\frac{{}_{ij}N}{BD} &= {}_{ij}\sigma_c\,{}_{ij}p_c - {}_{ii}\sigma_t\,{}_{ij}p_t \\ \frac{{}_{ij}M}{BD^2} &= {}_{ij}\sigma_c\,{}_{ij}p_c\left(\frac{1}{2}-{}_{ij}d_c\right)+{}_{ij}\sigma_t\,{}_{ij}p_t\left(\frac{1}{2}-{}_{ij}d_t\right)\end{aligned}\right\} \quad \cdots\cdots(8)$$

Equation 8 is applied to the ultimate strength method. In the superposition method, M-N interaction curve of reinforcing bars and steel with ideal I-section is obtained as the linear line elements passing through the points representing the ultimate load carrying capacity under pure thrust on the N-axis and the point representing the ultimate strength in pure flexure on the M-axis.

4.5 N and M in a Steel Web at the Ultimate State

The ultimate states of stress in a steel web are composed of a total of ten cases corresponding to the location of the neutral axis. The states of strain and stress in each case are shown in Fig. 7. The equations for the resultants N and M in a steel web or a steel portion with a rectangular cross section are developed hereafter.

(1) When $k \leq {}_{wj}d_c$

Case 1

$$\left.\begin{aligned}\frac{{}_{wj}N}{BD} &= \frac{1}{2}\cdot{}_{sj}E({}_{wj}\varepsilon_t-{}_{wj}\varepsilon_c)(1-{}_{wj}d_t-{}_{wj}d_c)\,{}_{wj}t_1 \\ \frac{{}_{wj}M}{BD^2} &= \frac{1}{2}\cdot{}_{sj}E(1-{}_{wj}dt-{}_{wj}d_c)\Big[{}_{wj}\varepsilon_c({}_{wj}d_t-{}_{wj}d_c) \\ &\quad +({}_{wj}\varepsilon_t+{}_{wj}\varepsilon_c)\left\{\frac{2}{3}(1-{}_{wj}d_t-{}_{wj}d_c)-\frac{1}{2}{}_{wj}d_c\right\}\Big]\,{}_{wj}t_1\end{aligned}\right\} \quad \cdots\cdots(9)$$

Case 2

$$\left.\begin{aligned}\frac{{}_{wj}N}{BD} &= \left\{-\frac{1}{2}({}_{wj}\sigma_y-{}_{wj}E\cdot{}_{wj}\varepsilon_c)\,Y-{}_{wj}\sigma_y(1-\sigma_y d_c-{}_{wj}d_t-x)\right\}{}_{wj}t_1 \\ \frac{{}_{wj}M}{BD^2} &= \Big\{{}_{wj}\sigma_y(1-{}_{wj}d_c-{}_{wj}d_t-Y)\,\frac{1}{2}(Y+{}_{wj}d_c-{}_{wj}d_t) \\ &\quad +\frac{1}{2}\cdot Y({}_{wj}\sigma_y+{}_{wj}E\cdot{}_{wj}\varepsilon_c)\left(\frac{2}{3}Y+{}_{wj}d_c-\frac{1}{2}\right) \\ &\quad -{}_{wj}E\cdot{}_{wj}\varepsilon_c\cdot Y\left(\frac{x}{2}+{}_{wj}d_c-\frac{1}{2}\right)\Big\}{}_{wj}t_1\end{aligned}\right\} \quad \cdots\cdots(10)$$

where, $Y=(k-{}_{wj}d_c)\left(1+\dfrac{{}_{wj}\varepsilon_y}{{}_{wj}\varepsilon_c}\right)$

Case 3

$$\left.\begin{aligned}\frac{{}_{wj}N}{BD} &= -{}_{wj}\sigma_y(1-{}_{wj}d_c-{}_{wj}d_t)\,{}_{wj}t_1 \\ \frac{{}_{wj}M}{BD^2} &= \frac{1}{2}\,{}_{wj}\sigma_y(1-{}_{wj}d_c-{}_{wj}d_t)({}_{wj}d_c-{}_{wj}d_t)\,{}_{wj}t_1\end{aligned}\right\} \quad \cdots\cdots(11)$$

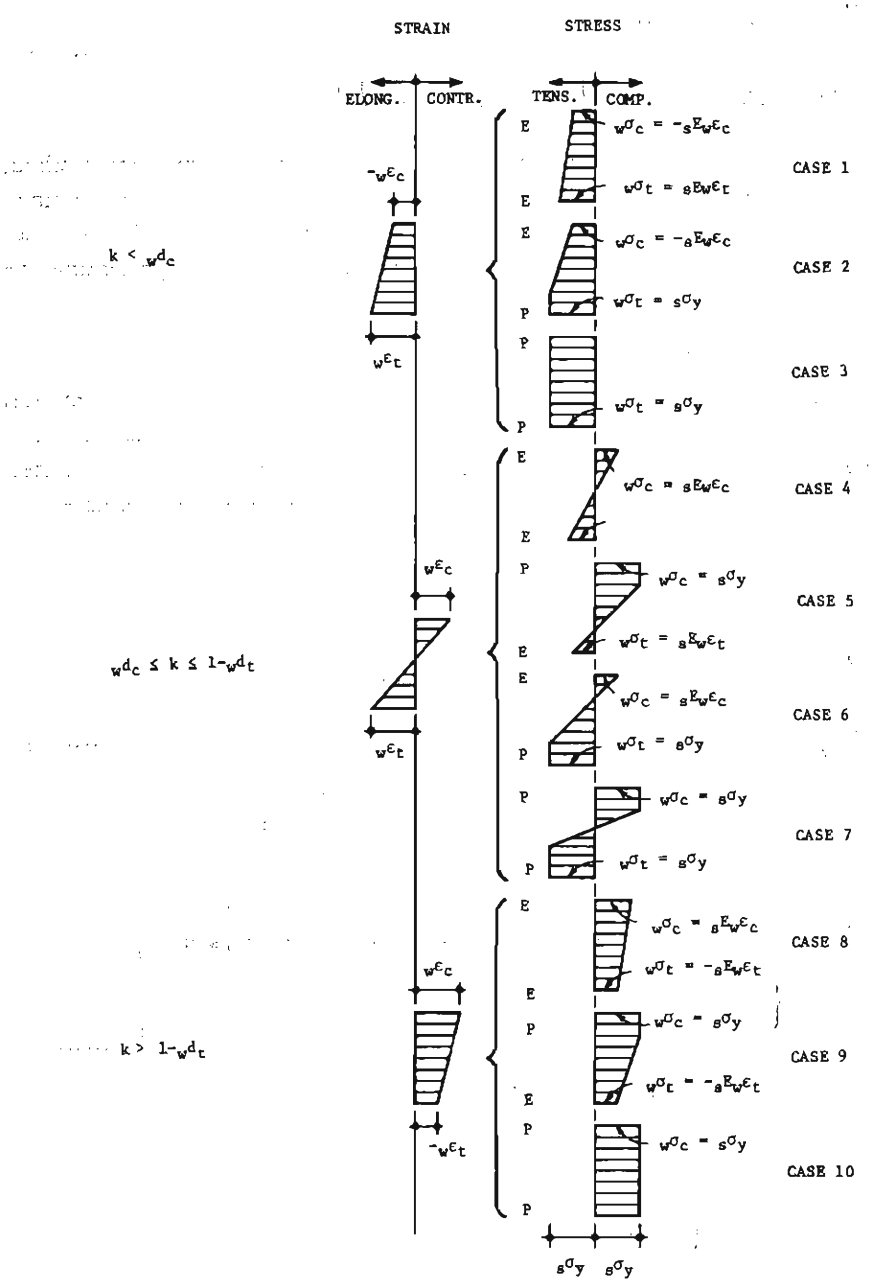

Fig. 7. Ultimate State of Steel Web.

(2) When $_{wj}d_c<k<1-{}_{wj}d_t$

Case 4

$$\left.\begin{aligned}\frac{{}_{wj}N}{BD} &= {}_{wj}n_1-{}_{wj}n_2\\ \frac{{}_{wj}M}{BD^2} &= {}_{wj}n_1\left\{\frac{1}{2}-{}_{wj}d_c-\frac{1}{3}(k-{}_{wj}d_c)\right\}\\ &\quad+{}_{wj}n_2\left\{\frac{1}{2}-{}_{wj}d_t-\frac{1}{3}(1-k-{}_{wj}d_t)\right\}\end{aligned}\right\} \quad\cdots\cdots(12)$$

where, $${}_{wj}n_1=\frac{1}{2}{}_{wj}\varepsilon_c(k-{}_{wj}d_c){}_{wj}E_{wj}t_1$$

$${}_{wj}n_2=\frac{1}{2}{}_{wj}\varepsilon_t(1-k-{}_{wj}d_t){}_{wj}E\cdot{}_{wj}t_1$$

Case 5

$$\left.\begin{aligned}\frac{{}_{wj}N}{BD} &= {}_{wj}n_1+{}_{wj}n_2-{}_{wj}n_3\\ \frac{{}_{wj}M}{BD^2} &= {}_{wj}n_1\left\{\frac{1}{2}-{}_{wj}d_c-\frac{1}{2}(k-{}_{wj}d_c)\left(1-\frac{{}_{wj}\varepsilon_y}{{}_{wj}\varepsilon_c}\right)\right\}\\ &\quad+{}_{wj}n_2\left\{\frac{1}{2}-{}_{wj}d_c-(k-{}_{wj}d_c)\left(1-\frac{{}_{wj}\varepsilon_y}{{}_{wj}\varepsilon_c}\right)-\frac{1}{3}\frac{{}_{wj}\varepsilon_y}{{}_{wj}\varepsilon_c}(k-{}_{wj}d_c)\right\}\\ &\quad+{}_{wj}n_3\left\{\frac{1}{2}-{}_{wj}d_t-\frac{1}{3}(1-k-{}_{wj}d_t)\right\}\end{aligned}\right\} \quad\cdots(13)$$

where, $${}_{wj}n_1={}_{wj}\sigma_y(k-{}_{wj}d_c)\left(1-\frac{{}_{wj}\varepsilon_y}{{}_{wj}\varepsilon_c}\right){}_{wj}t_1$$

$${}_{wj}n_2=\frac{1}{2}{}_{wj}\sigma_y(k-{}_{wj}d_c)\frac{{}_{wj}\varepsilon_y}{{}_{wj}\varepsilon_c}{}_{wj}t_1$$

$${}_{wj}n_3=\frac{1}{2}{}_{wj}\varepsilon_t\cdot{}_{wj}E(1-k-{}_{wj}d_t){}_{wj}t_1$$

Case 6

$$\left.\begin{aligned}\frac{{}_{wj}N}{BD^2} &= {}_{wj}n_1-{}_{wj}n_2-{}_{wj}n_3\\ \frac{{}_{wj}M}{BD^2} &= {}_{wj}n_1\left\{\frac{1}{2}-{}_{wj}d_c-\frac{1}{3}(k-{}_{wj}d_c)\right\}\\ &\quad+{}_{wj}n_2\left\{k+\frac{2}{3}(1-k-{}_{wj}d_t)\frac{{}_{wj}\varepsilon_y}{{}_{wj}\varepsilon_t}-\frac{1}{2}\right\}\\ &\quad+{}_{wj}n_3\left\{\frac{1}{2}-{}_{wj}d_t-\frac{1}{2}(1-k-{}_{wj}d_t)\left(1-\frac{{}_{wj}\varepsilon_y}{{}_{wj}\varepsilon_t}\right)\right\}\end{aligned}\right\} \quad\cdots\cdots(14)$$

where, $${}_wj n_1 = \frac{1}{2}\,{}_wj\varepsilon_c \cdot {}_wjE(k-{}_wjd_c)\,{}_wjt_1$$

$${}_wj n_2 = \frac{1}{2}\,{}_wj\sigma_y(1-k-{}_wjd_t)\frac{{}_wj\varepsilon_y}{{}_wj\varepsilon_t}\cdot {}_wjt_1$$

$${}_wj n_3 = {}_wj\sigma_y(1-k-{}_wjd_t)\left(1-\frac{{}_wj\varepsilon_y}{{}_wj\varepsilon_t}\right){}_wjt_1$$

Case 7

$$\left.\begin{aligned}
\frac{{}_wjN}{BD} &= {}_wjn_1-{}_wjn_3\\
\frac{{}_wjM}{BD^2} &= {}_wjn_1\left\{\frac{1}{2}-{}_wjd_c-\frac{1}{2}(k-{}_wjd_c)\left(1-\frac{{}_wj\varepsilon_y}{{}_wj\varepsilon_c}\right)\right.\\
&\quad +{}_wjn_2\left\{\frac{1}{2}-{}_wjd_c-(k-{}_wjd_c)\left(1-\frac{{}_wj\varepsilon_y}{{}_wj\varepsilon_c}\right)-\frac{1}{3}(k-{}_wjd_c)\frac{{}_wj\varepsilon_y}{{}_wj\varepsilon_c}\right\}\\
&\quad +{}_wjn_2\left[\frac{1}{2}-{}_wjd_t-\left\{1-k-{}_wjd_t-\frac{{}_wj\varepsilon_y}{{}_wj\varepsilon_c}(k-{}_wjd_c)\right\}-\frac{1}{3}(k-{}_wjd_c)\frac{{}_wj\varepsilon_y}{{}_wj\varepsilon_c}\right]\\
&\quad \left.+{}_wjn_3\left[\frac{1}{2}-{}_wjd_t-\frac{1}{2}\left\{1-k-{}_wjd_t-\frac{{}_wj\varepsilon_y}{{}_wj\varepsilon_c}(k-{}_wjd_c)\right\}\right]\right.
\end{aligned}\right\} \quad (15)$$

where, $${}_wj n_1 = {}_wj\sigma_y(k-{}_wjd_c)\left(1-\frac{{}_wj\varepsilon_y}{{}_wj\varepsilon_c}\right){}_wjt_1$$

$${}_wj n_2 = \frac{1}{2}\,{}_wj\sigma_y\frac{{}_wj\varepsilon_y}{{}_wj\varepsilon_c}(k-{}_wjd_c)\,{}_wjt_1$$

$${}_wj n_3 = {}_wj\sigma_y\left\{1-k-{}_wjd_t-\frac{{}_wj\varepsilon_y}{{}_wj\varepsilon_c}(k-{}_wjd_c)\right\}{}_wjt_1$$

(3) When $k \geq 1-{}_wjd_t$

Case 8

$$\left.\begin{aligned}
\frac{{}_wjN}{BD} &= \frac{1}{2}({}_wj\varepsilon_c-{}_wj\varepsilon_t)(1-{}_wjd_c-{}_wjd_t)\,{}_wjE\cdot{}_wjt_1\\
\frac{{}_wjM}{BD^2} &= -{}_wj\varepsilon_t\cdot{}_wjE(1-{}_wjd_c-{}_wjd_t)\left\{\frac{1}{2}-{}_wjd_c-\frac{1}{2}(1-{}_wjd_c-{}_wjd_t)\right\}{}_wjt_1\\
&\quad +\frac{1}{2}({}_wj\varepsilon_c+{}_wj\varepsilon_t)\,{}_wjE(1-{}_wjd_c-{}_wjd_t)\left\{\frac{1}{2}-{}_wjd_c-\frac{1}{3}(1-{}_wjd_c-{}_wjd_t)\right\}{}_wjt_1
\end{aligned}\right\} \quad (16)$$

Case 9

$$\left.\begin{aligned}
\frac{{}_wjN}{BD} &= {}_wjn_1-{}_wjn_2\\
\frac{{}_wjM}{BD^2} &= {}_wjn_1\left\{\frac{1}{2}-\frac{1}{2}(1-{}_wjd_c-{}_wjd_t)\right\}+{}_wjn_2\left\{\frac{1}{2}-{}_wjd_t-\frac{1}{3}\frac{{}_wj\varepsilon_y+{}_wj\varepsilon_t}{{}_wj\varepsilon_c}(k-{}_wjd_c)\right\}
\end{aligned}\right\} \quad (17)$$

where, ${}_wj n_1 = {}_wj\sigma_y(1-{}_wj d_c-{}_wj d_t){}_wt t_1$

$${}_wj n_2 = \frac{1}{2}({}_wj\sigma_y+{}_wj\varepsilon_t\cdot{}_wj E)\frac{{}_wj\varepsilon_y+{}_wj\varepsilon_t}{{}_wj\varepsilon_c}(k-{}_wj d_e){}_wj t_1$$

Case 10

$$\left.\begin{aligned}\frac{{}_wj N}{BD} &= {}_wj\sigma_y(1-{}_wj d_c-{}_wj d_t){}_wj t_1\\ \frac{{}_wj N}{BD^2} &= \frac{1}{2}{}_wj\sigma_y(1-{}_wj d_c-{}_wj d_t)({}_wj d_t-{}_wj d_c){}_wj t_1\end{aligned}\right\}\quad\cdots\cdots(18)$$

Equations 9 to 18 are to be used in the ultimate strength method.

4.6 *M-N* Interaction of Steel Shape at the Ultimate State

The *M-N* interaction of steel portion which is used in the superposition method is as follows.

(1) when $k<{}_sj d_c$

$$\left.\begin{aligned}\frac{{}_sj N}{BD} &= -{}_sj\sigma_y({}_sj p_c+{}_sj p_t+{}_wj p)\\ \frac{{}_sj M}{BD^2} &= 0\end{aligned}\right\}\quad\cdots\cdots(19)$$

(2) when ${}_sj d_c\leq k\leq 1-{}_sj d_t$

$$\left.\begin{aligned}\frac{{}_sj N}{BD} &= {}_sj\sigma_y({}_sj p_c-{}_sj p_t)\\ &\quad+{}_wj\sigma_y\cdot{}_wj t_1({}_wj d_t-{}_wj d_c+2k-1)\\ \frac{{}_sj M}{BD^2} &= {}_sj\sigma_y\left\{{}_sj p_c\left(\frac{1}{2}-{}_sj d_c\right)+{}_sj p_t\left(\frac{1}{2}-{}_sj d_t\right)\right\}\\ &\quad+\frac{1}{2}{}_wj\sigma_y\cdot{}_wj t_1\{(k-{}_wj d_c)(1-k-{}_wj d_e)\\ &\quad+(k-{}_wj d_t)(1-k-{}_wj d_t)\}\end{aligned}\right\}\quad\cdots\cdots(20)$$

(3) when $k>{}_sj d_t$

$$\left.\begin{aligned}\frac{{}_sj N}{BD} &= {}_sj\sigma_y({}_sj p_c+{}_sj p_t+{}_wj p)\\ \frac{{}_sj M}{BD^2} &= 0\end{aligned}\right\}\quad\cdots\cdots(21)$$

5. Results of Computation

The *M-N* interaction curve based on the superposition method is obtained from the vector sum of the *M-N* interaction curves of each component put in an SRC cross

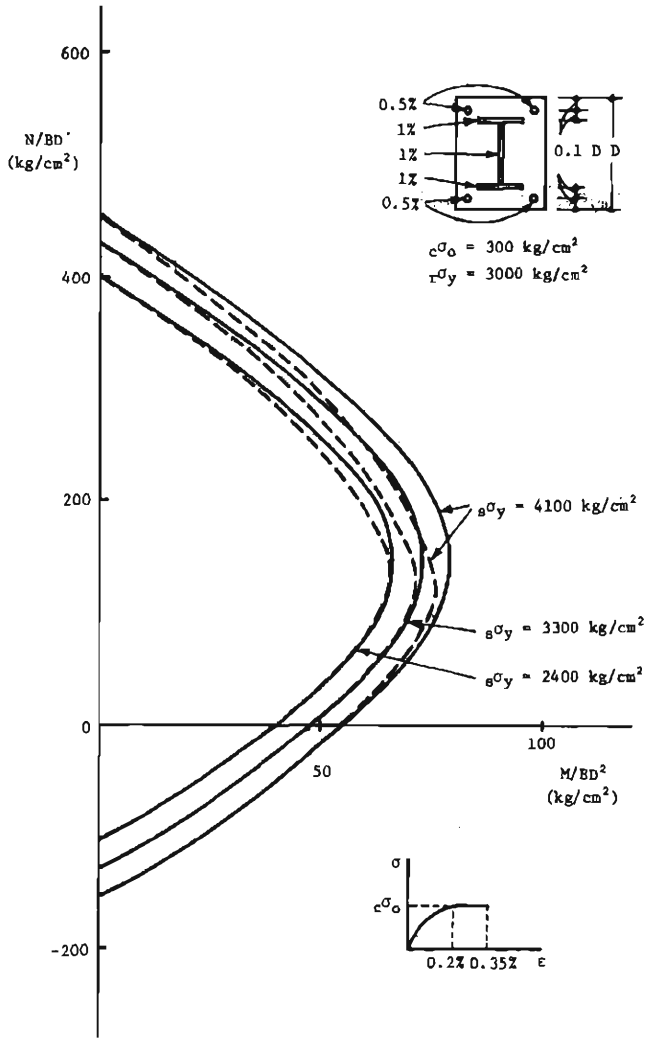

Fig. 8. Example of Computed Results.

section which is computed using the equations shown in the previous sections 4.3, 4.4 and 4.6. On the other hand, the *M-N* interaction curve based on the ultimate strength method is directly computed using the equations in sections 4.3, 4.4 and 4.5.[6] An example of computed results is shown in Fig. 8. Dashed lines are the results due to the ultimate strength method and solid lines are the ones due to the superposition method. In the figure, the ordinate and abscissa represent magnitudes of axial thrust and bending moment expressed in a dimension of stress, respectively.

5.1 Combination Use of Various Grades of Steel and Concrete

Figures 9 to 11 shows the effects of a variation of the yield stress of steel put in

a SRC section. The discrepancy between the results of two methods are very small for SS41 steel ($_s\sigma_y$=2400 kg/cm²) and SM50 steel ($_s\sigma_y$=3300 kg/cm²), for the case of SM58 steel ($_s\sigma_y$=4100 kg/cm²), it is a bit larger. Maximum error of the superposition method in that case is about 10%.

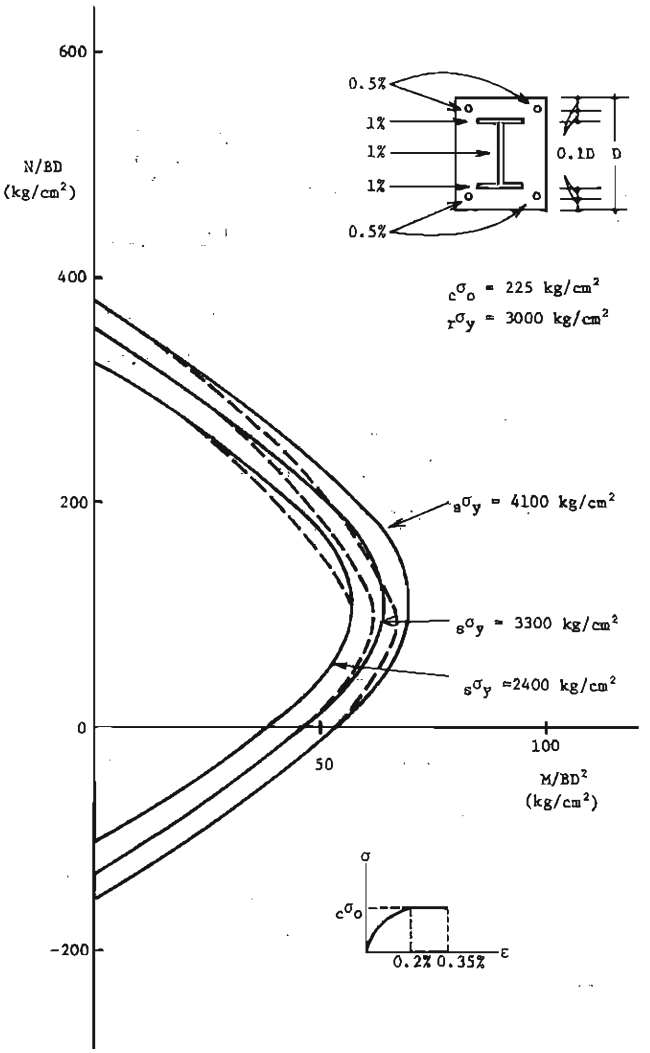

Fig. 9. Effects of Steel Strength (Strong Axis Bending).

Figure 12 shows the effects of variation of concrete strength in compression. The discrepancy between the two methods is also small. Such an amount of unsafe side error of the superposition method is sufficiently compensated for by the use of the reduced strength of concrete in the actual design procedure as shown in Fig. 13.

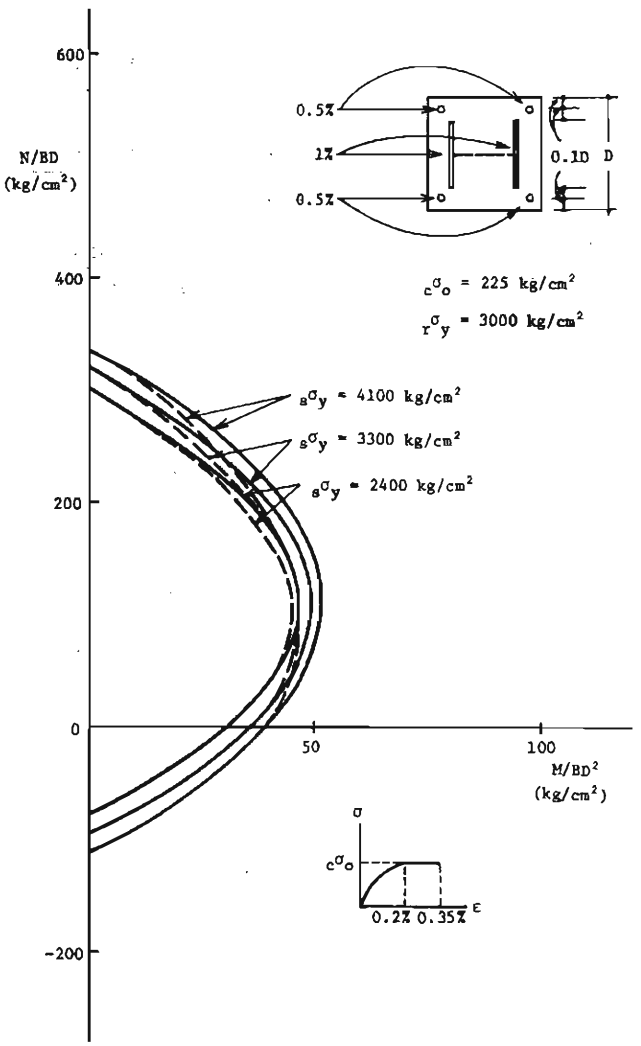

Fig. 10. Effects of Steel Strength (Weak Axis Bending).

5.2 Effects of the Depth of Steel Portion

Figure 14 shows the effects of the depth of steel portion in an SRC section. From the figure, it is understood that the error of the superposition method is pretty small even if a steel section with a small depth is put in a column section. Maximum

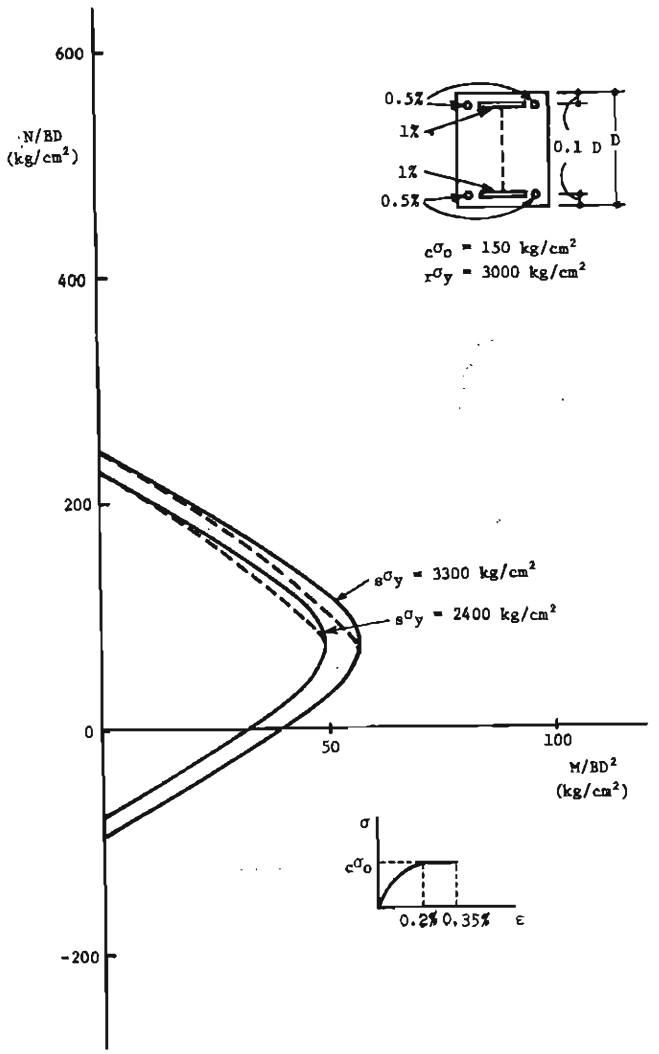

Fig. 11. Effect of Steel Strength ($_c\sigma_o$) = 150 kg/cm²).

unsafeside error of the superposition method is about 15% in comparison with the results of the ultimate strength method for the case where the depth ratio of the steel portion $a/D=0.2$.

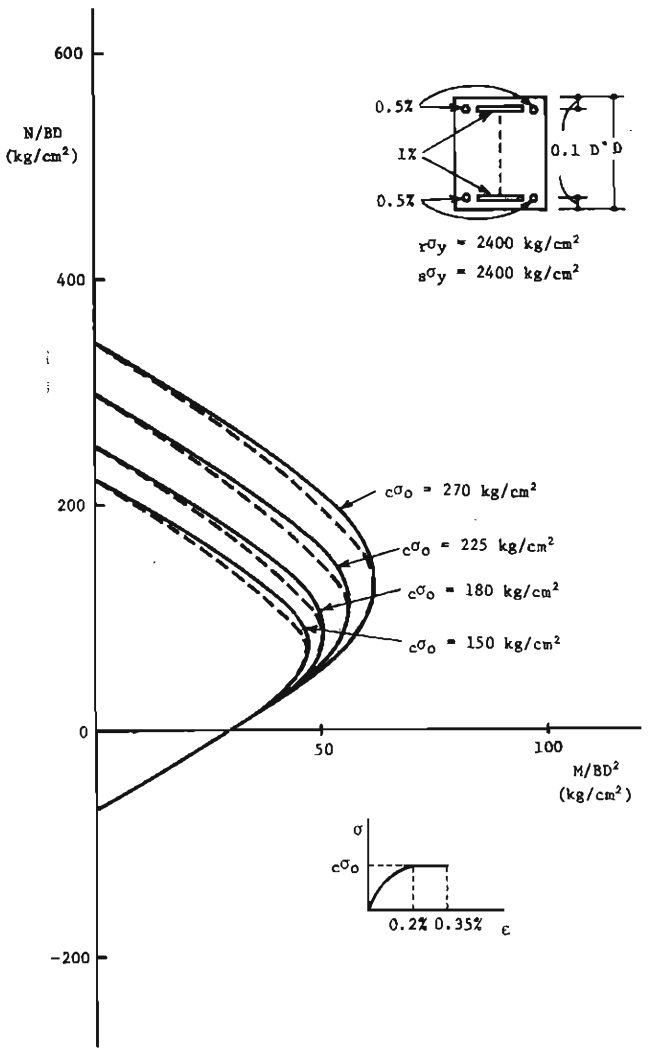

Fig. 12. Effects of Concrete Strength.

5.3 Effects of Crushing Strain of Concrete

Figures 15~21 show the effects of the crushing strain of concrete. If concrete crushes in too small range of strain in compression, the discrepancy between the two methods is pretty large (Figs. 17 and 18). However, when concrete performs in an

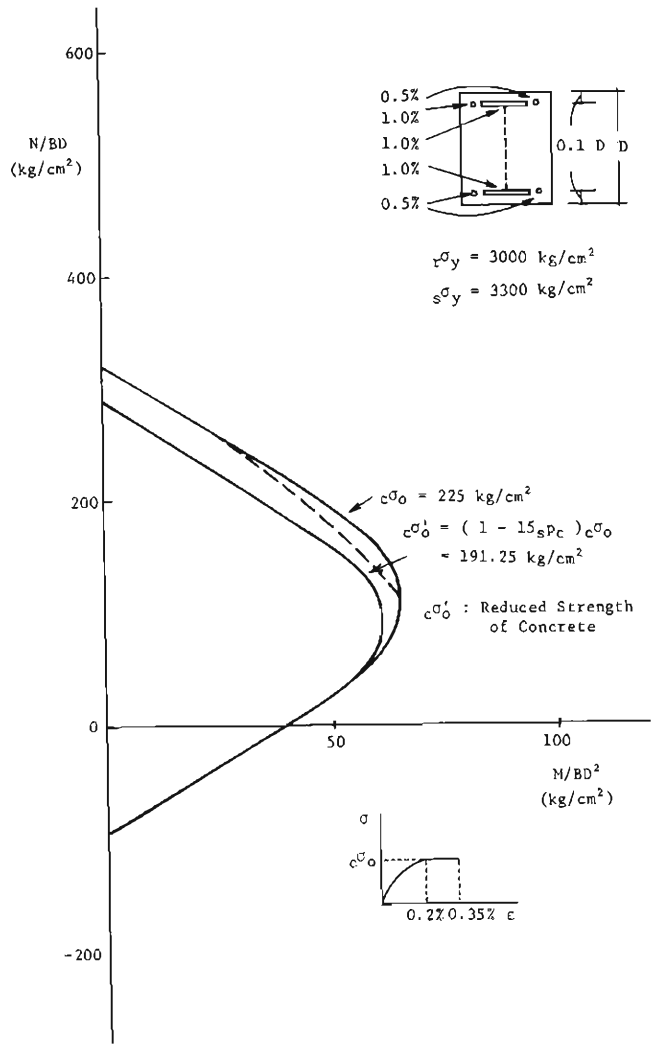

Fig. 13. Compensation of Unsafe-side Error of Superposition Method by Reduction of Concrete Strength.

ordinary manner in compression according to the reasonable stress-strain relationship (Figs. 9 and 15), the discrepancy is so small as to be able to be offset by the use of reduced strength of concrete. The reduced strength of concrete gives a quite conservative M-N interaction for an SRC cross section (see Fig. 13).

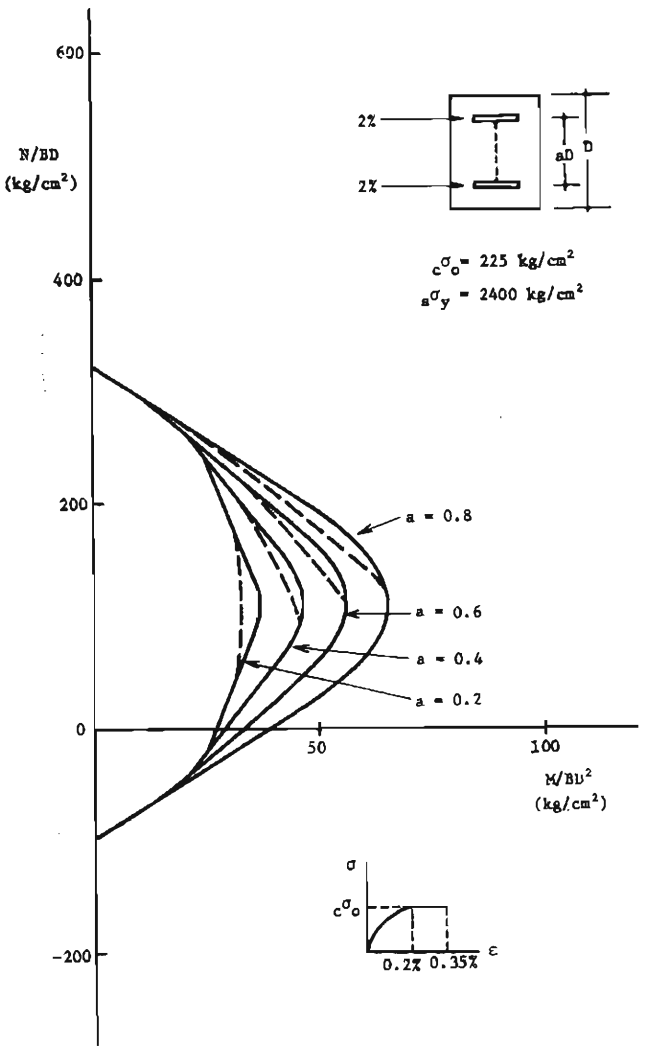

Fig. 14. Effects of Depth of Steel Portion.

5.4 Effects of the Amount of Steel Reinforcement

Figure 22 shows the effects of the amount of steel reinforcement in an SRC section. The discrepancy is also small.

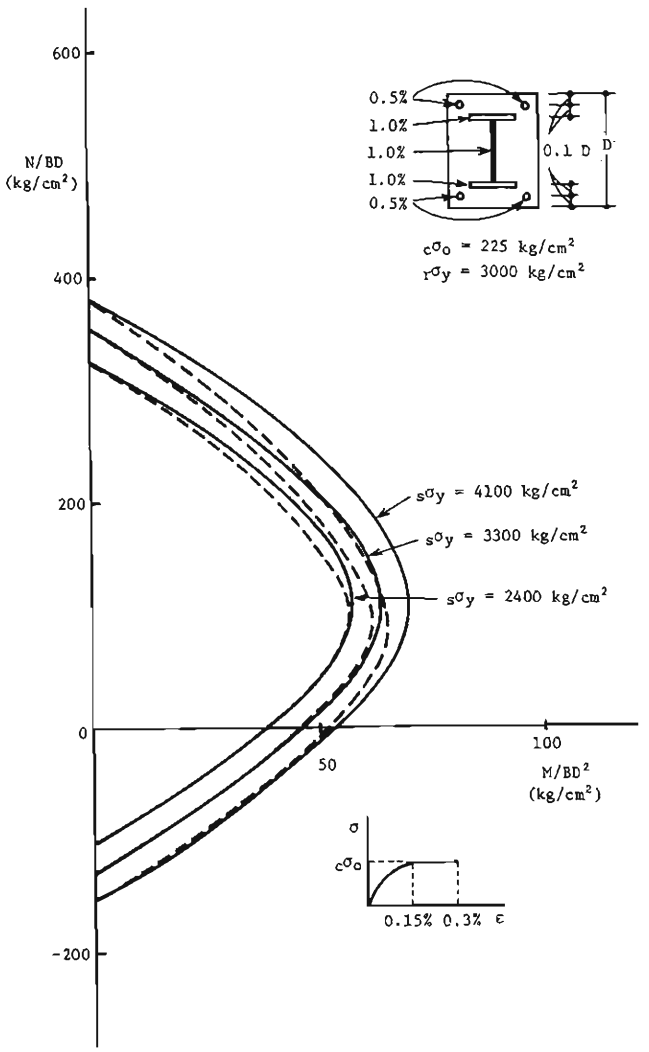

Fig. 15. Effects of Stress-Strain Relationship of Concrete—(I).

5.5 Effects of Asymmetrical Arrangement of the Steel Portion in Cross Section

An example of the effect of an ansymmetrical arrangement of the steel portion is shown in Fig. 23. The discrepancy between the two methods is not so large as

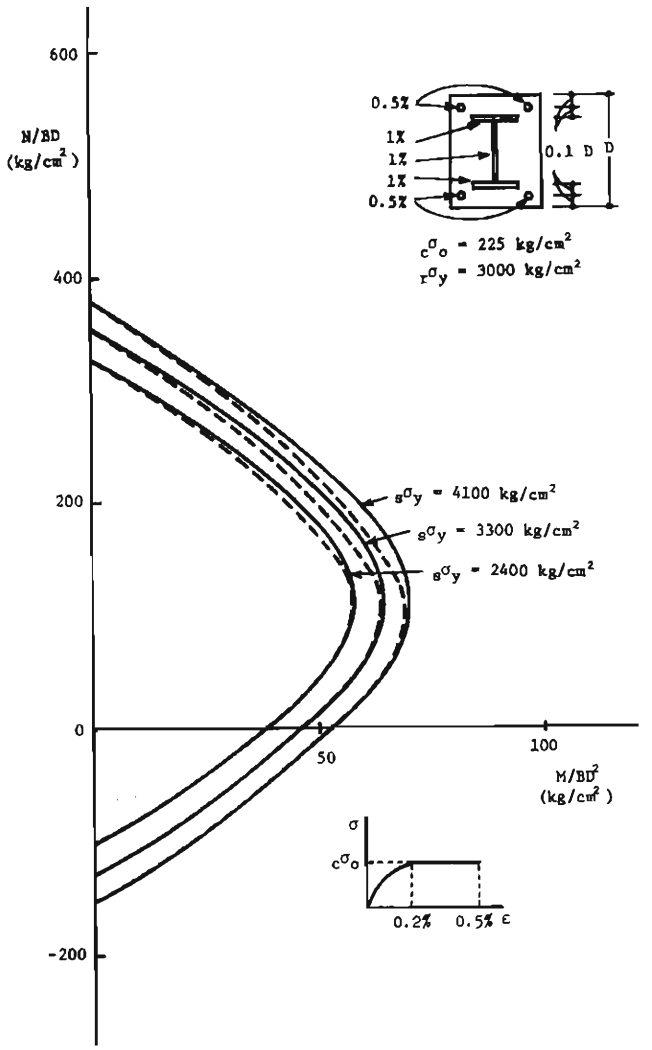

Fig. 16. Effects of Stress-Strain Relationship of Concrete—(II).

to be worried about the asymmetrical steel portion.

6. Concluding Remarks

It is concluded based on the computed results that the superposition method gives

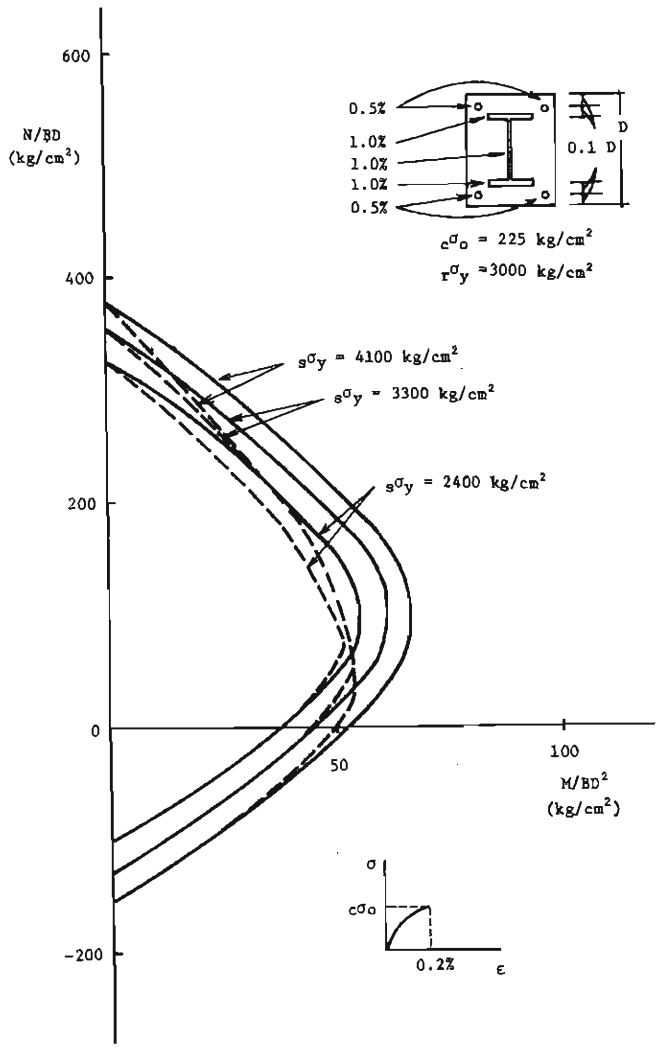

Fig. 17. Effects of Stress-Strain Relationship of Concrete—(III).

a good approximation of the ultimate load carrying capacity of SRC column section under the combination use of various grades of concrete and ordinary grades of steel. The arrangement of the steel portion in a cross section and amount of steel reinforcement do not affect very much the accuracy of the superposition method to estimate

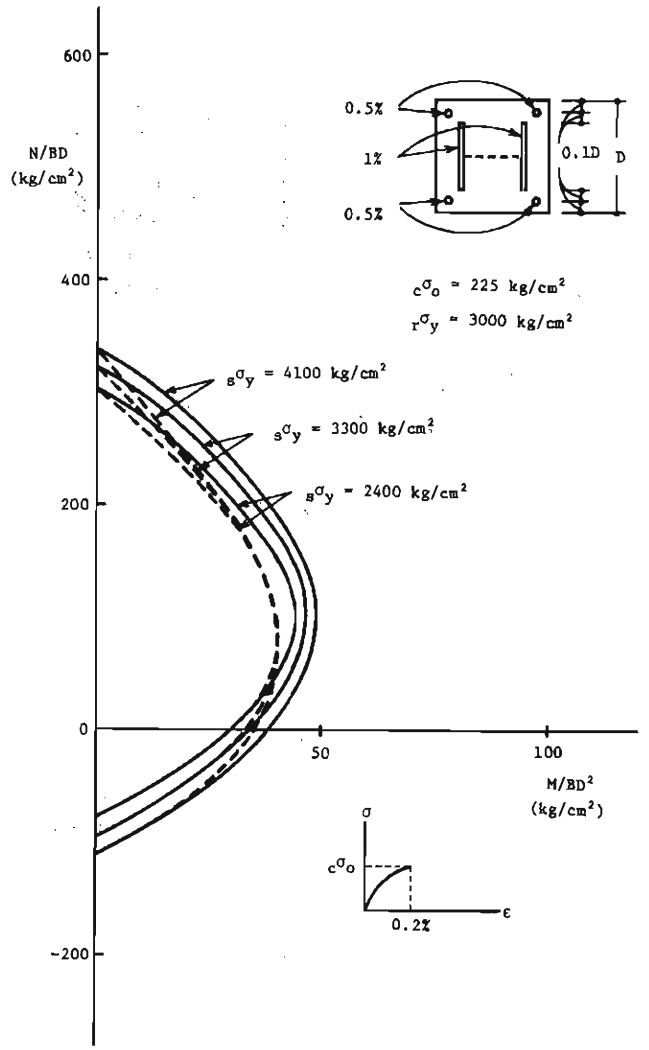

Fig. 18. Effects of Stress-Strain Relationship of Concrete—(IV).

the ultimate strength of an SRC column section.

The "Superposition Method" is an appropriate and simple method to estimate the ultimate load carrying capacity of the steel reinforced concrete column section subjected to axial thrust and bending moment simultaneously, unless the steel with too

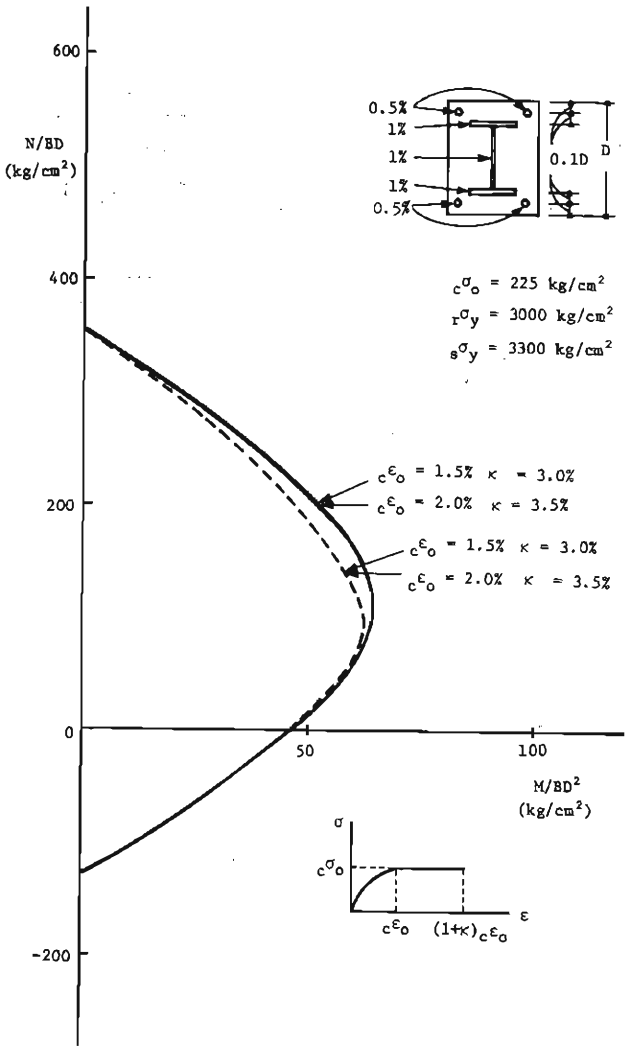

Fig. 19. Effects of Stress-Strain Relationship of Concrete—(V).

high yield strength is used in a design. The unsafeside error in the superposition method is able to be sufficiently compensated for by using a reduced strength of concrete.

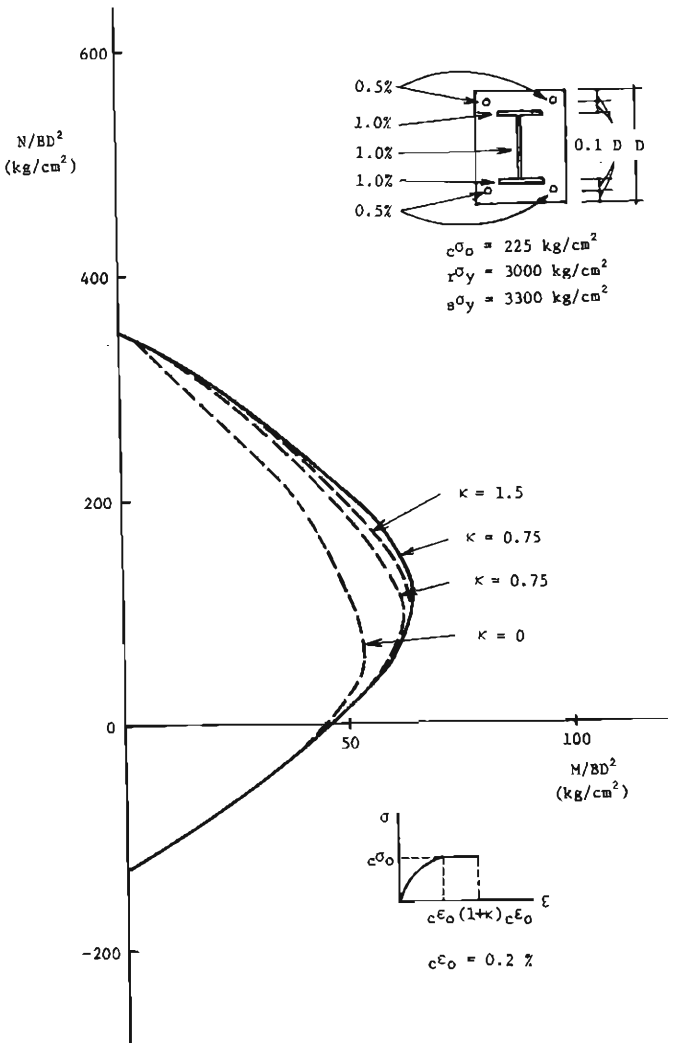

Fig. 20. Effects of Stress-Strain Relationship of Concrete—(VI).

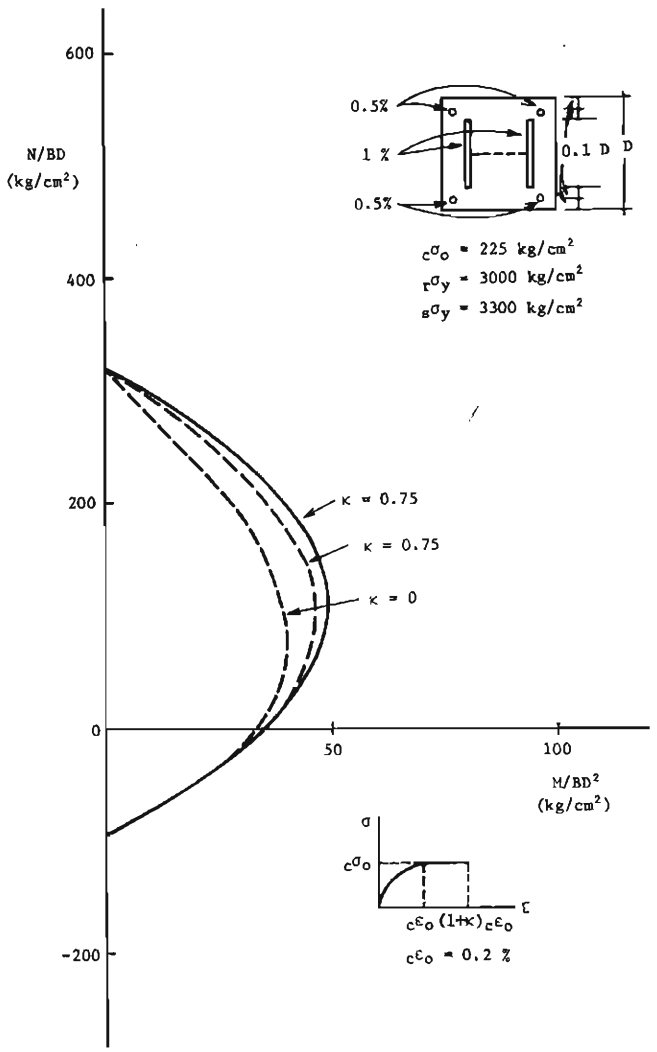

Fig. 21. Effects of Stress-Strain Relationship of Concrete—(VII).

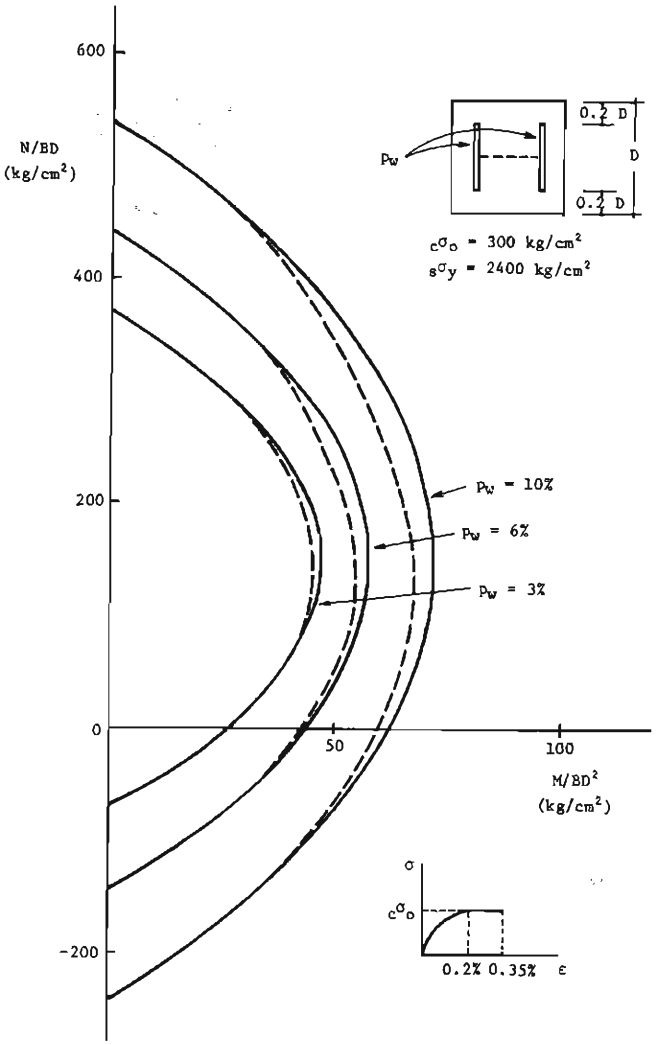

Fig. 22. Effects of Amount of Steel.

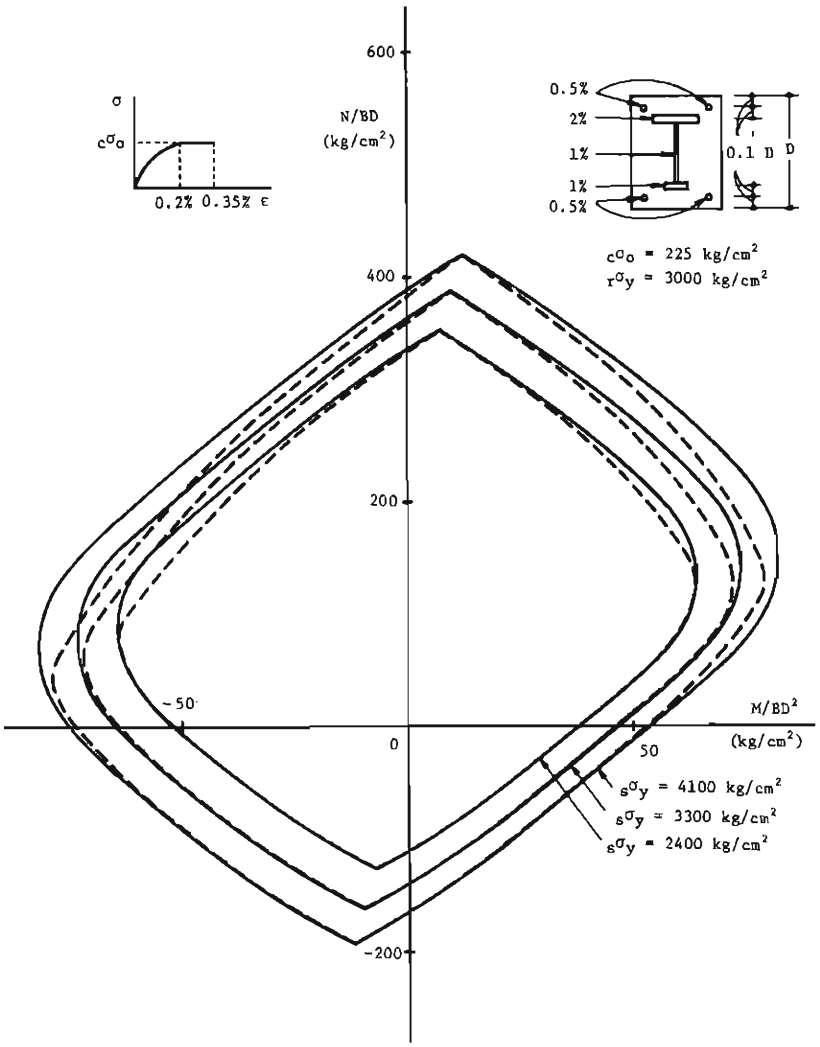

Fig. 23. Results for Ansymmetrical Steel Portion.

Nomenclature

${}_{ij}a_c$: cross sectional area of main compressive reinforcement in i-component in j-th layer

${}_{ij}a_t$: cross sectional area of main tensile reinforcement in i-component in j-th layer

B : width of cross section of column

D : depth of cross section of column

${}_sE$: Young's modulus of steel

${}_{ij}E$: Young's modulus of i-component in j-th layer

F_c : ultimate stress of concrete

i : prefix denotes section component, $i=r, s, w$

j : prefix denotes layer number

k : non-dimensionalized location of neutral axis

M : bending moment

M_c : bending moment in concrete

${}_{ij}M$: bending moment in i-component in j-th layer of steel

N : axial thrust

N_c : axial thrust in concrete

${}_{ij}N$: axial thrust in i-component in j-th layer of steel

${}_{wj}n_k$: sub-variables

${}_{ij}p_c$: reinforcement ratio in compression side

$$ {}_{ij}p_c = \frac{{}_{ij}a_c}{BD} $$

${}_{ij}p_t$: reinforcement ratio in tension side

$$ {}_{ij}p_t = \frac{{}_{ij}a_t}{BD} $$

${}_{wj}p$: web reinforcement ratio

SRC : steel reinforced concrete

${}_{wj}t$: thickness of web in j-th layer

${}_{wj}t_1$: non-dimensionalized web thickness in j-th layer

$$ {}_{wj}t_1 = \frac{{}_{wj}t}{B} $$

ε : fiber strain

${}_c\varepsilon_B$: crushing strain of concrete

$$ {}_c\varepsilon_B = (1+\kappa)_c\varepsilon_0 $$

${}_c\varepsilon_0$: yield strain of concrete

${}_{ij}\varepsilon_c$, ${}_{ij}\varepsilon_t$: fiber strain of i-component in j-th layer

${}_{ij}\varepsilon_y$: yield strain of i-component in j-th layer

${}_s\varepsilon_y$: yield strain of steel

κ : variable which denotes the length of plastic range of concrete

σ : longitudinal stress

${}_c\varepsilon_y$: ultimate stress of concrete

${}_{ij}\sigma_c$, ${}_{ij}\sigma_t$: stress in i-component in j-th layer

${}_{ij}\sigma_y$: yield stress of i-component in j-th layer

References

1) Wakabayashi, M., S. Takada and H. Saito: Steel Reinforced Concrete Structures, Structural Engineering Series (Kenchiku Kozogaku Taikei), Vol. 19, 1967, Shokokusha (Tokyo), pp. 32–72 (in Japanese).

2) Wakabayashi, M., et al.: Steel Reinforced Concrete Structures, Architectural Engineering Series (Kenchikugaku Taikei), Vol. 18, 1970, Shokokusha (Tokyo), pp. 242–273 (in Japanese).

3) Tanaka, H.: Study on Additional Strength Theory, Transactions of AIJ, No. 57, July 1957, pp. 261–264 (in Japanese).

4) Hirano, M.: Additional Strength of Cross Sections and that of Structures, Transactions of AIJ, No. 63, October 1959, pp. 397–400 (in Japanese).